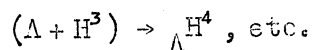
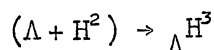


R. Levi-Setti,

Enrico Fermi Institute, University of Chicago.

I. BASIC DEFINITIONS AND NOMENCLATURE

$\Lambda$  hypernucleus: a hyperon bound to a nuclear core



The nuclear core need not be a stable nucleus; examples of hypernuclei in which the core in its ground state is a nuclear resonant state are e.g.  $(\Lambda + Be^8) \rightarrow \Lambda Be^9$ , where ordinary  $Be^8$  would disintegrate  $Be^8 \rightarrow 2He^4 + 0.1 \text{ MeV}$ . Occasionally the  $\Lambda$ -nucleon attraction provides sufficient binding to form hypernuclei out of a completely unbound core, e.g.  $(\Lambda + Be^6) \rightarrow \Lambda Be^7$  where ordinarily  $Be^6 \rightarrow 2p + He^4 + 1.4 \text{ MeV}$ .

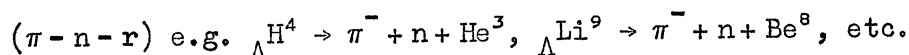
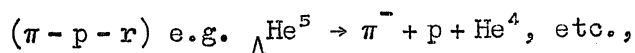
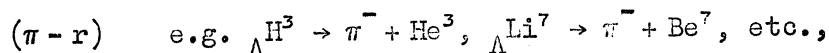
The  $\Lambda$ -binding energy  $B_\Lambda$  is defined as usual from

$$\Lambda(A, Z) = (A-1, Z) + \Lambda - B_\Lambda \quad (1)$$

and can be measured, since  $\Lambda(A, Z) \rightarrow \sum_{ij} (\Lambda_i, Z_j) + Q$

$$B_\Lambda = Q_0 - Q, \text{ where } Q_0 = (A-1, Z) + \Lambda - \sum_{ij} (\Lambda_i, Z_j). \quad (2)$$

Hypernuclear disintegrations in which  $\Lambda \rightarrow \pi^- + p$  are called mesonic decays; those where  $\Lambda + n, p \rightarrow n + n, p$  are called non-mesonic decays. Common abbreviations for decay modes are



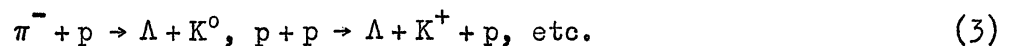

---

\*) This paper was also presented at the Hyperfragment Conference.

Note that  $Q_0$  for  $(\pi, p, r)$  decays is always  $Q_\Lambda = 37.58$  MeV.  $B_\Lambda$  can be measured best from mesonic or mesic decays in view of the low energy release, usually in the range 25 - 55 MeV. For non-mesic decays  $Q \approx 176$  MeV -  $B_\Lambda$ .

## II. OBSERVATION AND IDENTIFICATION OF HYPERNUCLEI

Although hyperfragments can originate any time a  $\Lambda$  is created within a nucleus, and therefore from reactions such as



the most copious source of h.f. are  $K^-$  induced reactions in nuclear matter, where the elementary reactions are



The reason is obvious; while reactions of type (3) have a high threshold and small cross-section, reactions of type (4) are exothermic and occur very frequently. The big step of creating strangeness is separated, in Eq. (4), from that of producing h.f.'s. Typical production rates of h.f.'s from  $K^-$  absorbed at rest in light nuclei are  $\sim 2 - 5\%$ . In the processes of production, survival and decay of a hyperfragment we find the means of observation and identification of particular hypernuclear species. It would be desirable, of course, to be able to compare the observables on the three steps simultaneously. This is, however, seldom possible.

### 1. Identification at production

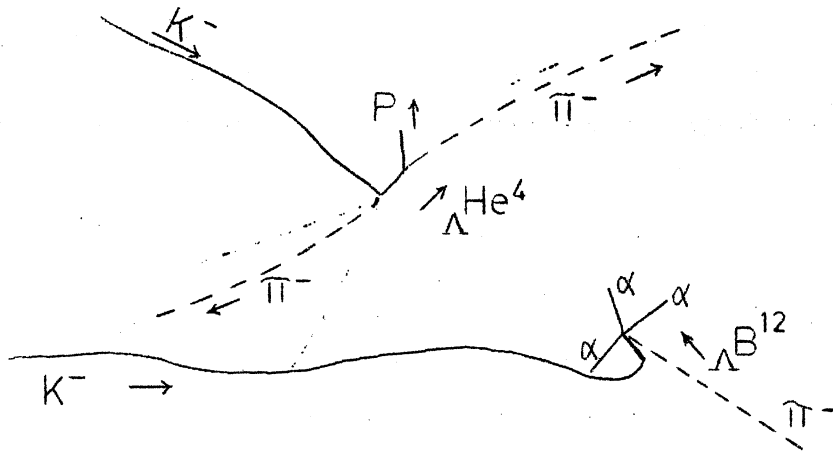
Identification at production is particularly reliable in two-body reactions



These reactions are obviously exclusive domain of the He bubble chamber. Similar reactions have been observed in nuclear emulsion, such as:



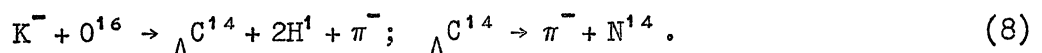
Fig.1



In this case, however, the uncertainty as to the target nucleus detracts from the evidence. The requirements of energy and momentum balance can only be checked approximately in Eq. (6), where the only observable of the production process is a very short ( $\sim 4 \mu\text{m}$ ) h.f. track. Hopefully, reactions such as in lithium-loaded emulsion should yield an independent clear-cut identification at production



Occasionally it is possible to obtain a satisfactory energy, momentum, charge and mass balance of more complicated production reactions in nuclear emulsion. Very seldom, however, is such information independent from that supplied by the decay process. This method is in all cases a very powerful tool; very likely the only method to give a reliable identification of relatively heavy hypernuclei. As we shall see, some decay modes ( $\pi$ -r) of heavy hypernuclei become completely non-characteristic and a combined analysis of production and decay reaction is called for, e.g.



Related remark The use of small emulsion stacks for h.f. work prevents, in general, the observation of the production pion in its entire range, and its sign determination. On the other hand, at this stage in h.f. work, this information is quite fundamental.

## 2. Identification during survival

Hyperfragments can be identified during their survival namely from measurements on the h.f. track itself. If the h.f. comes to rest and it has sufficient range, any of the conventional means of determining mass and charge in emulsion apply. Thus, direct mass measurements can occasionally identify  $\Lambda^3$  and  $\Lambda^4$  when several millimeters of track are available. Z determinations usually require more than  $\sim 50 \mu\text{m}$  of h.f. track to be reliable. Thickness measurements in various ways, as well as gap-length measurements have been used. A direct determination of Z often determines the identity of a h.f., when its decay offers certain alternatives, e.g. for  $\Lambda^4$ ,  $\Lambda^4$ , when in the  $\pi$ -p-r mode of decay the recoil has a very short range, insufficient for direct distinction from range-momentum curves. Identification from h.f. decay is still the most widely attained.

## 3. Identification at decay

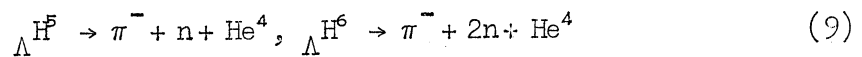
A blind approach to this problem is that of feeding input data, such as ranges and angles into a computer programmed to try all permutations of prong identities until a good fit is obtained. Then, amongst the output reactions, one chooses the one which yields the lowest momentum unbalance  $\Delta P$ . Although this procedure is necessary for the analysis of complicated decays, it may often hide some relevant information. Thus, a few remarks are in order.

( $\pi$ -r) events

The pion momentum uniquely determines the recoil momentum and comparison with P-R curves immediately identifies the event. This is true, of course, for recoils which are long enough to afford discrimination.

In order to improve the fit, collinearity may be imposed, when justified. The direction of the recoil is, in fact, seldom well defined, in particular its dip angle. One can obtain a better recoil range estimate by measuring its projected range, and inferring its dip angle from the knowledge of the  $\pi$  direction.

Note This is a procedure which should be used with caution. There is a point in measuring accurately  $\Delta P$  and deviations from collinearity even for species as common and typical as  $\Lambda H^4 \rightarrow \pi^- + He^4$ . In fact, if species such as  $\Lambda H^5$ ,  $\Lambda H^6$  should exist, their decays



could very well simulate  $\Lambda H^4 \rightarrow \pi^- + He^4$ , with some departure from collinearity. Furthermore, a decay

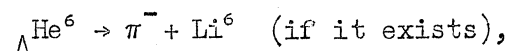


would look like an anomalous  $\pi$ -r decay of  $\Lambda H^4$ , with a recoil somewhat shorter ( $\sim 5.4 \mu m$ ) than usual ( $8.1 \mu m$ ).

Some of the possible pitfalls in identifying  $\pi$ -r events are worth mentioning. Even  $\Lambda H^3 \rightarrow \pi^- + He^3$  is not exempt from simulators. In fact,



can occur in a configuration similar to  $\Lambda H^3$  ( $\pi$ -r). In such a case, however, the h.f. track should tell the difference unless too short (as usually the case for  $\Lambda Li^9$ ). The real difficulties arise from  $\pi$ -r decays of heavier species, when the discriminating power of the recoil range is lost (as well as the possibility of ascertaining collinearity!). The trouble begins very soon. We are very likely unable to tell the difference between



and



Both decays yield (or are expected to)  $\pi$  ranges of  $\sim 2.2$  cm and recoil ranges in the neighbourhood of  $2 \mu\text{m}$ . If  $\Lambda\text{He}^8$  should exist, its decay

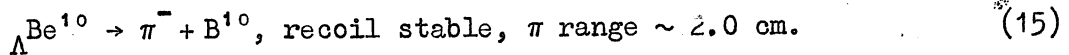
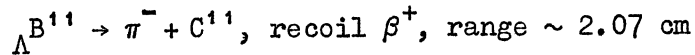


would have an overwhelming chance of being confused with



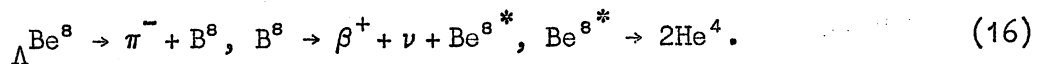
From  $\Lambda\text{Be}^{10}$  on, all recoils have a range of  $1 \mu\text{m}$  or less. On the other hand, the  $\pi$  ranges from many different species overlap. The properties of the recoils may then help, like their  $\beta$  decay

See fig. 2



The failure to observe the decay  $\beta$  will automatically involve misidentification. Even when the recoil is unstable like  $\text{Li}^8$ , a pitfall is open. Take

See fig. 3



If the  $\beta^+$  were overlooked, the event may be interpreted in a very complicated way, perhaps even as



The same would hold for a hypothetical decay



All this is further complicated by the possibility that heavy recoils be emitted in excited states, or that the hypernucleus decays from an isomeric state. For these reasons, identifications based on  $\pi$ -r events of heavy h.f. should always be taken with great caution and in general are not as clear-cut as those based on other all-charged decay modes. The importance of a combined analysis production-decay vertices for these events cannot be stressed any further.

( $\pi$ -p-r) events

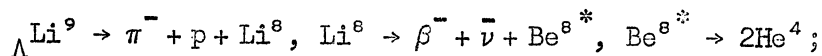
After checking for consistency with coplanarity, it is, in general, useful to impose coplanarity by inferring the recoil direction from that of the resultant momentum  $\vec{P}_{\pi p} = \vec{P}_{\pi} + \vec{P}_p$ . Next it is useful to plot  $|\vec{P}_{\pi p}|$  versus the corrected recoil range  $R_{rec}$ . Range momentum curves can be constructed experimentally in this way for various isotopes. Errors and anomalies can easily be spotted. Below certain recoil ranges it becomes impossible to discriminate among neighbouring isotopes. Thus, below  $\sim 3 \mu\text{m}$ , it becomes meaningless to accept a discrimination between  $\text{He}^3$  and  $\text{He}^4$ . Problem cases of this type are frequently encountered for all species,  ${}_{\Lambda}^3\text{H}$ ,  ${}_{\Lambda}^4\text{H}$ ,  ${}_{\Lambda}^4\text{He}$ ,  ${}_{\Lambda}^5\text{He}$ ,  ${}_{\Lambda}^7\text{Li}$ , etc. For the lighter species, however, a good fraction of the events yield recoils in the sensitive region. For the heavier species, problem cases become the rule because the recoil ranges, usually very short, become increasingly insensitive to the momentum  $\vec{P}_{\pi p}$ . Obviously in this region, one cannot even assess that the decay is indeed of the  $\pi$ -p-r type, nor that neutrons are emitted. Analysis in conjunction with the production kinematics becomes once more crucial. In discussing  $\pi$ -p-r events of even the lighter hypernuclei, one should bear in mind that the recoil co-ordinates in the P-R plot have considerable spread. In certain regions

See fig. 4

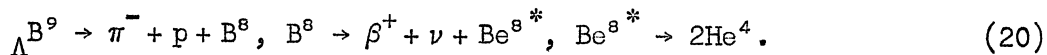
of the plot, in particular when an abundant species ( ${}_{\Lambda}^5\text{He}$ ) is next to a less abundant one ( ${}_{\Lambda}^4\text{He}$ ) some overlap of the distributions will always occur, so that some contamination of one species with another may be present. With increased statistics one can attempt to purify a collection of events of a given species by imposing a progressively increasing range cut-off on the recoil in order to accept events only in a region of the (P-R) plots where no overlap can occur.

Remark A procedure as outlined above is the only method to eliminate from a sample of a given species possible contaminations. Such contaminations introduce systematic biases in the determination of, for example, binding energies. The addition of small or large samples of identified h.f. to the world statistics becomes a worthless proposition if only  $B_{\Lambda}$ 's or worse,  $\bar{B}_{\Lambda}$ 's are given. The raw data are instead needed in order to attempt an elimination of the intrinsic, systematic errors due to contamination.

Again, some features of the recoil may help, when the recoil itself is too short. For example, in the decay



watch out, however, for the very similar decay

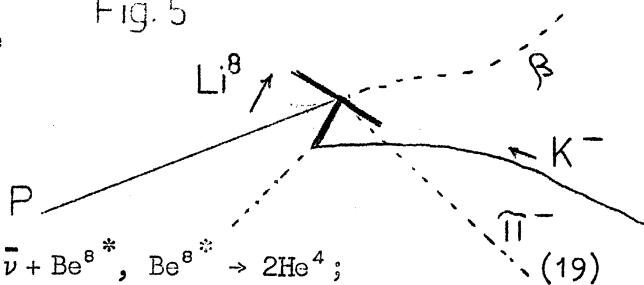


Incidentally, the range energy curves obtained from h.f. recoil in nuclear emulsion are quite certainly the best available in the approximate range 2 - 40  $\mu\text{m}$ .

( $\pi$ -n-r) and complex decays

These events are best analysed with computer programmes. However, the following example illustrates some auxiliary method to improve the over-all reliability in the identification of a certain class of events.

Fig. 5





The decay



may easily be confused with



when the neutron momentum is  $|\vec{P}_n| \leq 40 \text{ MeV}/c$ . The  $\Delta P$  distribution for three-body charged decays, in fact, extends up to this approximate value, due to measurement errors. If the energy release  $Q$  is plotted against the missing momentum  $P_n$  (or  $\Delta P$ ), a separation between  ${}_{\Lambda}^8\text{Li}$  and  ${}_{\Lambda}^9\text{Li}$  can be achieved on an entire body of events, and some statistical method may be used to cut off a possible contamination of  ${}_{\Lambda}^8\text{Li}$  events amongst  ${}_{\Lambda}^9\text{Li}$ . See fig.6

A general comment is required concerning all decays involving neutron emission, when considering  $B_{\Lambda}$ . Such events will yield systematically underestimates of  $B_{\Lambda}$ . In fact, while the momentum unbalance  $\Delta P$ , due to exp. errors is neglected in decays involving only charged particles,  $\Delta P$  will contribute to the estimate of the neutron momentum, as

$$(P_n)_{\text{exp}} = (P_n)_{\text{true}} + \frac{(\Delta P)^2}{3(P_n)_{\text{true}}} \quad (23)$$

Thus, the neutron energy will be overestimated, and so will  $Q$ , giving a corresponding underestimate of  $B_{\Lambda}$ . Of course, this effect will be felt at small ( $P_n \approx \Delta P$ ) neutron momenta and is in general small. However, since average  $B_{\Lambda}$ 's for some species, or even individual decay modes, have errors (statistical) smaller than 0.1 MeV, even an effect of this kind should not be neglected. Whenever possible, it may be best to base binding energy estimates on decay modes involving charged particles only.

#### 4. Identification on the basis of $B_{\Lambda}$

This is the last remedy, resort to which is obviously very dangerous. It is difficult, of course, to assess the extent to which it is practiced. To some extent it is always used, if nothing else, when one rejects an identification leading to a negative  $B_{\Lambda}$ . It should be realized, however, that an identity, giving a  $B_{\Lambda}$  in agreement with a known value is by no means an identification. Pitfalls may be wide open when a species is "expected" to have a certain  $B_{\Lambda}$ , and an event is attributed to that species on this basis. This is particularly the case with  $(\pi - r)$  events, where the interpolated  $B_{\Lambda}$  is the only basis on which to predict the configuration. The only situation in which this approach seems justified is encountered in the determination of branching ratios between various decay modes of a certain species, e.g. the separation between the  $(\pi - p - r)$  decays of  ${}_{\Lambda}H^3$  and  ${}_{\Lambda}H^4$ , when the recoil is invisible. Careless use of this method will, on the other hand, produce non-Gaussian distributions of  $B_{\Lambda}$ , will cut off interesting tails, and will hide possible splittings in  $B_{\Lambda}$  due to excited initial or final states.

#### 5. Experiments with known target nuclei

Some have been mentioned previously. It may be that even accurate  $B_{\Lambda}$  estimates may be obtained from the measurement of the  $\pi$  range following



where  $Q = B_{\Lambda} - B_n + 176$  MeV, and  $B_n$  is the binding of the last neutron in  $(A, Z)$ . This approach carries the identification at production to its logical extreme, that of producing particular h.f. species. It may be valuable for  $A \gtrsim 8 - 10$ . It offers the advantage that techniques other than nuclear emulsion may be used advantageously, such as bubble chambers, spark chambers, etc.

### III. INFORMATION DERIVED FROM HYPERNUCLEAR PROPERTIES

What does one learn from the study of hypernuclei, study which is based so far on a sample of perhaps 2000 mesic decays analysed in nuclear emulsion and several hundreds in the He bubble chamber? Several basic answers have been given to properties of the strong and weak interaction of the  $\Lambda$  hyperon with nucleons, as well as to intrinsic questions regarding strange particles properly.

A brief summary of the main results is the following.

#### 1. Strong $\Lambda$ -n interaction

a) The  $\Lambda$ -nucleon interaction is charge symmetric as substantiated by the well-established existence of hypernuclear charge multiplets. Such multiplets correspond to those for the nuclear cores since the  $\Lambda$  has isospin  $T = 0$ .

b) The  $\Lambda$ -nucleon interaction is strong with coupling constant of the order of unity. This follows from an analysis of the  $\Lambda$ -binding energies for light hypernuclei. A measure of this strength is given (following Dalitz) by the volume integral of a  $\Lambda$ -nucleon central potential of appropriate shape for a particular spin state  $S$ . In these terms one can compare the  $\Lambda$ -n to the  $n$ - $n$  interaction, e.g.

$${}^3S_1 \text{ n-p volume integral } U \approx 1400 \text{ MeV } f^3$$

$${}^1S_0 \text{ } \Lambda\text{-p volume integral } U \approx 380 \text{ MeV } f^3.$$

Since the range of  $\Lambda$ -nucleon force is much shorter (at least two  $\pi$  exchange) than that of the  $n$ - $n$  force, the over-all  $\Lambda$ - $n$  binding is weaker than the corresponding nucleon-nucleon binding, even though the interactions have comparable strengths<sup>1)</sup>. Alternatively, the interaction can be described in terms of singlet and triplet scattering lengths. (See Dalitz, following lecture.)

c) The  $\Lambda$ -nucleon interaction is strongly spin-dependent. This follows from an analysis of both the  $\Lambda$ -binding energies and the direct determination of the spin of several hypernuclei ( ${}_{\Lambda}^3\text{H}$ ,  ${}_{\Lambda}^4\text{H}$ ,  ${}_{\Lambda}^8\text{Li}$ ). Indirect information stems also from the measurement of hypernuclear lifetimes. The  ${}^1\text{S}_0$   $\Lambda$ -n interaction is more attractive than that in the  ${}^3\text{S}_1$  state, opposite to the nucleon-nucleon case<sup>2)</sup>.

For the sake of illustration, recall that the Fermi scattering lengths are, for:

n-p

$$a_s = -2.34 \times 10^{-12} \text{ cm}$$

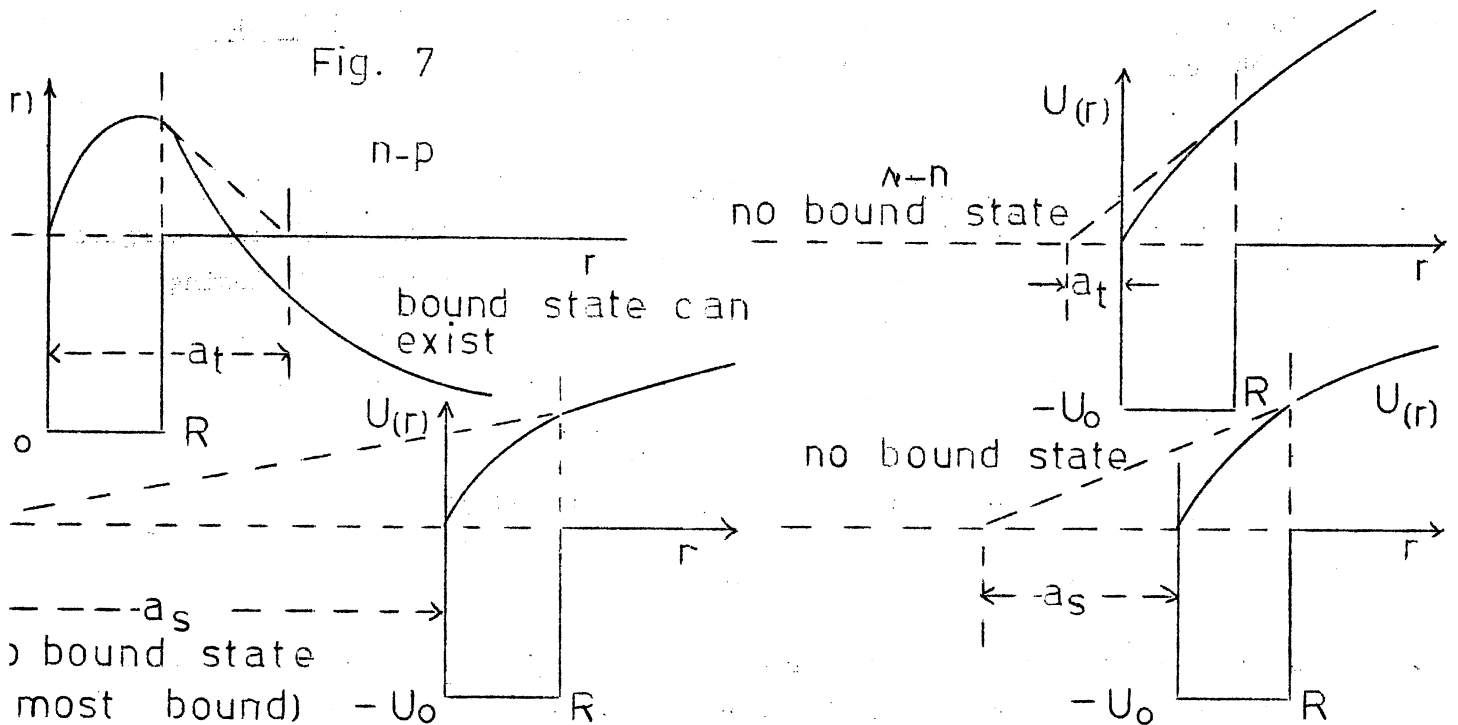
$$a_t = 0.52 \times 10^{-12} \text{ cm}$$

$\Lambda$ -p (See Dalitz, next lecture).

$$a_s \approx -2.4 \times 10^{-13} \text{ cm}$$

$$a_t \approx -0.6 \times 10^{-13} \text{ cm}$$

Fig. 7



d) The well-depth experienced by a  $\Lambda$  particle in nuclear matter is  $\approx 30$  MeV. This result stems from the determination of  $B_{\Lambda}$  for heavy hypernuclei as well as from theoretical calculations.

e) The  $K^-$  is a pseudoscalar particle. This follows the study of the reaction  $K^- + \text{He}^4 \rightarrow {}_{\Lambda}^4\text{H} + \pi^0$  in the He bubble chamber, knowing that  $J({}_{\Lambda}^4\text{H}) = 0$ .

## 2. Weak $\Lambda$ -n interaction

- a) Several checks of the validity of the  $|\Delta T| = 1/2$  rule in  $\Lambda$ -pionic decay modes have been given from the study of branching ratios in the decay modes of some light hypernuclei. Perhaps the most significant result is the determination of the ratio  $p_0/s_0$  between the p- and s-wave amplitudes in  $\Lambda$ -decay via the  $\pi^0$  mode obtained by the He bubble chamber group. The prediction of the  $|\Delta T| = 1/2$  rule, that  $p_0/s_0 = p/s$  seems well satisfied.
- b) Information on the strength of the weak interaction leading to  $\Lambda + n \rightarrow n + n$ . This is obtained from the branching ratios non-mesic/mesic for the decay modes of individual hypernuclear species. Very little is known on this subject. One would like to know whether, for instance, this interaction is spin-dependent or not.

## 3. Nuclear physics

A variety of final state interaction effects can be found in hypernuclear decays. Typical examples  ${}_{\Lambda}\text{He}^5 \rightarrow \pi^- + \text{Li}^{5*}$ ;  $\text{Li}^{5*} \rightarrow p + \text{He}^4$  ( $P_{3/2}$  resonance dominant)  ${}_{\Lambda}\text{Li}^8 \rightarrow \pi^- + \text{Be}^{8*}$ ;  $\text{Be}^{8*} \rightarrow \pi^- + 2\text{He}^4$  ( $0^+$ ,  $2^+$  intermediate states present). These properties, as we shall see, may be very useful for specific purposes, like spin determination. Occasionally, new information on low energy nuclear physics problems may be gained as a by-product.

We will now try to justify some of the above results by presenting the evidence in some detail.

## IV. $\Lambda$ BINDING ENERGIES

The enclosed tabulation contains up-to-date averages of  $B_{\Lambda}$  for established species. When relevant,  $\bar{B}_{\Lambda}$  are given separately for the most abundant decay modes of the same species. Several features are exhibited by a plot of  $B_{\Lambda}$  versus mass number A.

See fig.8

These are:

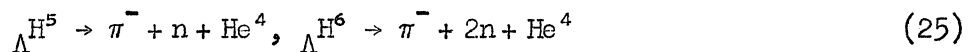
- i) the presence of charge multiplets reflecting the isospin structure of the core nuclei;
- ii) an over-all monotonic increase of  $B_{\Lambda}$  as a function of A;
- iii) a discrete structure within the multiplets which is to be attributed to spin-dependent effects.

${}_{\Lambda}^3\text{H}$  is the lightest hypernucleus known. It is attributed  $T = 0$  since there is no evidence for the other members of a  $T = 1$  state,  ${}_{\Lambda}^3\text{n}$  and  ${}_{\Lambda}^3\text{He}$ . Its  $B_{\Lambda}$  is very small,  $(0.31 \pm 0.15)$  MeV and the  $B_{\Lambda}$  distribution for this species is rather broad, somewhat more than expected from range-straggling alone.

See fig.9

$\Lambda^4$ ,  $\Lambda^4$  are mirror hypernuclei ( $T = 1/2$ ) and have very similar  $B_\Lambda$ 's ( $2.14 \pm 0.08$ ) MeV and ( $2.47 \pm 0.09$ ) MeV respectively as required from charge symmetry. One may comment that these values, due to the small errors, are almost in disagreement. The  $\bar{B}_\Lambda$  determination of  $\Lambda^4$  requires some more detailed investigation. As can be seen from Table 1,  $\pi^-$ -r events yield for  $\bar{B}_\Lambda$  the value ( $2.40 \pm 0.12$ ) MeV, very close to  $\Lambda^4$ . n events give a very low  $\bar{B}_\Lambda$ , ( $1.75 \pm 0.1$ ) MeV and perhaps should not be included in the average for the reasons discussed above. Finally, ( $\pi^-$ -p-r) events for which  $\bar{B}_\Lambda = (2.00 \pm 0.14)$  MeV could contain a contamination of  $\Lambda^3$  which would lower  $\bar{B}_\Lambda$ . On the other hand,  $\Lambda^4$  could well contain a contamination of  $\Lambda^5$ , which would increase  $\bar{B}_\Lambda$ , in the sense of emphasizing a difference between  $\Lambda^4$  and  $\Lambda^4$  which may not be real at all. The one way to improve the situation here is not a mere increase in statistics, but a more severe selection of the events as pointed out in the section on identification problems.

The  $B_\Lambda$  distribution for the  $\pi^-$ -r decays of  $\Lambda^4$  is somewhat skew at the higher end. This could be due on one side to the inclusion of events in which the long pion (4 cm) may have lost energy in undetected interactions. On the other hand, a contamination of still hypothetical decays:



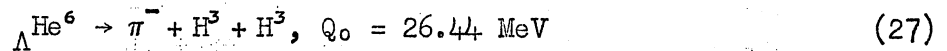
cannot be ruled out and should perhaps be kept in mind.

$\Lambda^5$ . It is the most abundant hypernucleus. It decays essentially by the  $\pi^-$ -p-r mode only. Its  $\bar{B}_\Lambda$ , ( $3.10 \pm 0.05$ ) MeV, is the best known and the  $B_\Lambda$  distribution is the closer to a Gaussian than any of the others.

( $\Lambda^6$ ,  $\Lambda^6$ ). No clear cut evidence for the existence of these hypernuclei has been reported, nor the large number of  $\Lambda^5$  giving decays also compatible with



is a valid argument to support the existence of  $\Lambda^6\text{He}$ . The decay



would provide good evidence.

See fig.10

$\Lambda^7\text{He}$ ,  $\Lambda^7\text{Li}$ ,  $\Lambda^7\text{Be}$ .  $\Lambda^7\text{Li}$  has  $T = 0$  while  $\Lambda^7\text{He}$  and  $\Lambda^7\text{Be}$  are members of a  $T = 1$  state. The  $B_\Lambda$  for  $\Lambda^7\text{Li}$  is well-established,  $(5.52 \pm 0.12)$  MeV from decays other than  $\pi$ -r. Only two examples of  $\Lambda^7\text{Be}$  are known, yielding  $\bar{B}_\Lambda = (4.9 \pm 0.5)$  MeV while for  $\Lambda^7\text{He}$  an average of 14  $B_\Lambda$  values would give  $\bar{B}_\Lambda = (3.96 \pm 0.24)$  MeV.

See fig.11



Two effects are present here. On one side, the  $\bar{B}_\Lambda$  of  ${}_\Lambda\text{Li}^7$  is higher than either of the  $\bar{B}_\Lambda$  of  ${}_\Lambda\text{He}^7$  or  ${}_\Lambda\text{Be}^7$ , and this can be understood in terms of the spin dependence of the  $\Lambda$ -nucleon interaction. On the other side, the  $\bar{B}_\Lambda$ 's for  ${}_\Lambda\text{He}^7$  and  ${}_\Lambda\text{Be}^7$  which should be identical, are indeed in disagreement. A suggestion made by Danysz and Pniewski<sup>3)</sup>, is the following.  ${}_\Lambda\text{He}^7$  may decay from an isomeric state ( $\text{He}^6$  has a level at 1.6 MeV in the continuum) and the observed  $B_\Lambda$  distribution may contain, in fact, two groups of  $B_\Lambda$ 's. That this should be the case is substantiated by the very existence of  ${}_\Lambda\text{Be}^7$ . In fact, the condition for the stability of  ${}_\Lambda\text{Be}^7$  against break up



is that its  $B_\Lambda$  be greater than 4.5 MeV. Thus even with only two  ${}_\Lambda\text{Be}^7$  events, we know that  $B_\Lambda({}_\Lambda\text{Be}^7)$  must exceed 4.5 MeV. From charge symmetry one would then expect that the ground state  ${}_\Lambda\text{He}^7$  should have  $B_\Lambda$  also  $> 4.5$  MeV. Thus, considerable interest is attached to an increase in the statistics of  ${}_\Lambda\text{He}^7$  events. At present it is difficult to detect a splitting in the  $B_\Lambda$  distribution. The reasons to expect such splitting are, however, plausible, as will be further illustrated by Dalitz (these lectures).

${}_\Lambda\text{Li}^8, {}_\Lambda\text{Be}^8$ . Another well-established pair of mirror hypernuclei. Their  $\bar{B}_\Lambda$ 's are in very close agreement.

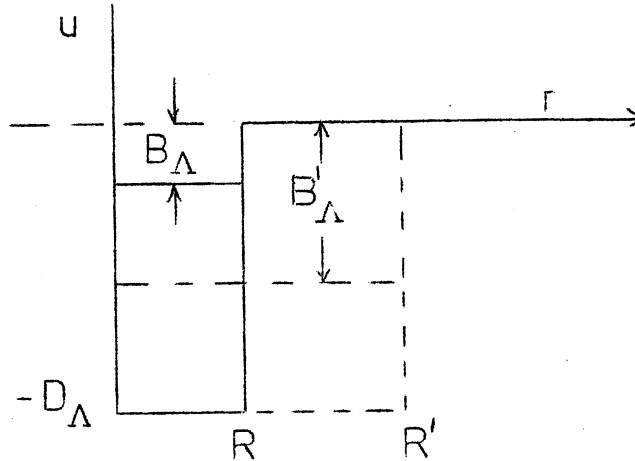
See fig.12

$\Lambda$ Li<sup>9</sup>,  $\Lambda$ Be<sup>9</sup>, ( $B^9$ ). The binding energy of  $\Lambda$ Li<sup>9</sup> (T = 1) is about 1.5 MeV greater than that of  $\Lambda$ Be<sup>9</sup> (T = 0). This is of course a point of great interest because if this difference is to be attributed to spin dependence only, it may be incompatible with the results from the mass 7 hypernuclei. Unfortunately the  $B_\Lambda$  distribution for  $\Lambda$ Li<sup>9</sup> is not one of the most satisfactory.  $\Lambda$ B<sup>9</sup> has never been reported. Its decay ( $\pi$ -p-r) could be confused, as remarked before, with that of  $\Lambda$ Li<sup>9</sup>. This misidentification would not, however, affect the observed large difference in  $B_\Lambda$  between the T = 0 and T = 1 states. For heavier species, the plot shows how little is known. The spread  $\sigma$  of the  $B_\Lambda$  distributions is shown as a function of Q in the following plot. The over-all monotonic increase of  $B_\Lambda$  versus A can be understood in a rather simple way. The  $\Lambda$  particle, not obeying the Pauli principle in a single  $\Lambda$  hypernucleus, occupies the lowest s state. Thus, no saturation effects are expected until the  $\Lambda$  will reach the bottom of the potential well, for a very heavy hypernucleus.

See fig. 13

As the radius R of the region of interaction increases, with increasing A, the  $\Lambda$  will progressively "sink" to a lower energy state in the well. This can be seen as follows. Consider for simplicity the  $\Lambda$  in a square potential well of depth  $U(r) = -D_\Lambda$ , radius R.

Fig. 14



The standard solution of the Schrödinger equation for this problem, after matching the wave functions at the boundary R is:

$$K \cot KR = -\gamma, \text{ or } \sqrt{\frac{2M}{\hbar^2} (D_\Lambda - B_\Lambda)} \cot \sqrt{\frac{2M}{\hbar^2} (D_\Lambda - B_\Lambda)} R = -\sqrt{\frac{2M}{\hbar^2} B_\Lambda} \quad (29)$$

$$\cot \sqrt{\frac{2M}{\hbar^2} (D_\Lambda - B_\Lambda)} R = -\sqrt{\frac{B_\Lambda}{D_\Lambda - B_\Lambda}}. \quad (30)$$

One can now find approximate solutions for convenient asymptotic cases. Take for example  $B_\Lambda \approx D_\Lambda$ , then

$$\sqrt{\frac{2M}{\hbar^2} (D_\Lambda - B_\Lambda)} R \approx \pi; \quad B_\Lambda \approx D_\Lambda - \frac{\pi^2 \hbar^2}{2M_\Lambda r_0^2 A^{2/3}}. \quad (31)$$

Equation (31) expresses explicitly how  $B_\Lambda$  depends on A for heavy hypernuclei. This equation suggests a method for the determination of  $D_\Lambda$ . In fact, a plot of  $B_\Lambda$  versus  $A^{-2/3}$  for heavy hypernuclei should be, in the zeroth approximation, a linear plot. Extrapolation to  $A \rightarrow \infty$  will give a value for  $D_\Lambda$ . This has indeed been accomplished at least partially from the knowledge of an upper limit of  $B_\Lambda$  for hypernuclei in the mass range  $60 < A < 100$ . The result<sup>4)</sup> is that  $D_\Lambda \lesssim 30$  MeV. The upper limit of  $B_\Lambda$  for  $60 < A < 100$  hypernuclei was obtained from the upper limit in the energy release of mesic and non-mesic disintegrations of "spallation hyperfragments".

See fig.15

An attempt is being made at present to obtain a lower limit of  $B_{\Lambda}$  for bromine hypernuclei following the measurement of the energy release in the reaction at rest



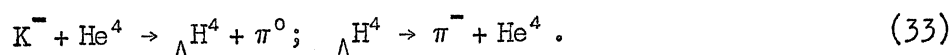
if such a reaction is found to occur to the ground state or some low lying state of  ${}_{\Lambda}Br^{79}$ . This study is made in a large  $CF_3Br$  bubble chamber where  $K^{-}$  mesons have been brought to rest. Even when  $B_{\Lambda}$  for heavy hypernuclei is known more accurately, the crude linear extrapolation to  $D_{\Lambda}$  will have to be improved, making use of a better approximation of Eq. (31). This will take into account a more realistic shape for the potential and indications are (Dalitz) that the correct functional dependence of  $B_{\Lambda}$  versus  $A^{-2/3}$  is not linear but possesses some curvature (the slope increases slightly with A).

## V. THE SPINS OF $\Lambda$ HYPERNUCLEI

Spin assignments have been obtained so far for  $\Lambda^3\text{H}$ ,  $\Lambda^4\text{H}$ , and  $\Lambda^8\text{Li}$ . The spin of species with spinless core, such as  $\Lambda^5\text{He}$  can be inferred as being equal to the  $\Lambda$  spin,  $J = 1/2$ . We can distinguish several approaches to this problem.

- i) Determination by direct methods. It implies the production or selection of an aligned sample of hypernuclei. It is based on the study of angular correlations of the decay products with respect to some axis of quantization.
- ii) Determination from branching ratios of different decay modes. Conservation of angular momentum may favour certain final states over others.
- iii) More indirect approaches, e.g. based on hypernuclear lifetimes. These are, however, not independent of (ii).

Take, for example,  $\Lambda^4\text{H}$ . A direct spin determination has been obtained by the He bubble chamber group from a study of the sequence of reactions



All particles in these reactions are spinless except possibly  $\Lambda^4\text{H}$  which can have at the most  $J = 0$  or  $1$ . If  $\Lambda^4\text{H}$  has  $J = 0$ , the decay  $\Lambda^4\text{H} \rightarrow \pi^- + \text{He}^4$  is then necessarily isotropic. Note that in such a case, since the orbital angular momentum  $l$  in the initial state must equal the orbital angular momentum  $L$  in the final state, the observation of Eq. (33) implies that the intrinsic parity  $\omega_{\text{K}} = \omega_{\pi} = -1$  or ( $\omega_{\Lambda} = +1$  by convention) that the K is pseudoscalar. Consider now the case of  $J = 1$ , and  $\text{K}^-$  capture from an s-orbital (there are good arguments in favour of this assumption<sup>5</sup>). Then  $L = 1$  in the final state which implies that  $\omega_{\text{K}} = +1$ , a scalar K meson. As to the angular distribution in the decay of  $\Lambda^4\text{H}$ , take the direction of  $\Lambda^4\text{H}$  as the axis Z of quantization. Only the projection  $J_Z = m(\Lambda^4\text{H}) = 0$  is allowed in the final state.

YPA2000

This, in turn, implies that in the rest system of  $\pi$ ,  $\text{He}^4$ ,  $l_\pi = 1$ ,  $m_\pi = 0$ . Then the angular distribution is characterized by the spherical harmonic  $Y_1^0(\theta)$  only and  $P(\theta) \propto \cos^2 \theta$ . The exp. distribution found by Block et al.<sup>6)</sup>

is isotropic, strongly suggesting that  $J(\Lambda^0) = 0$  and that the K is pseudoscalar. Prior to this direct determination,  $J = 0$  for  $\Lambda^0$  had already been assigned as a result of an emulsion experiment.

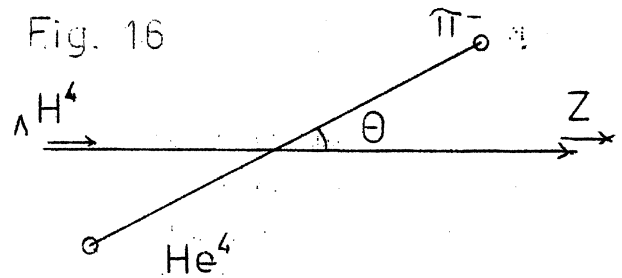
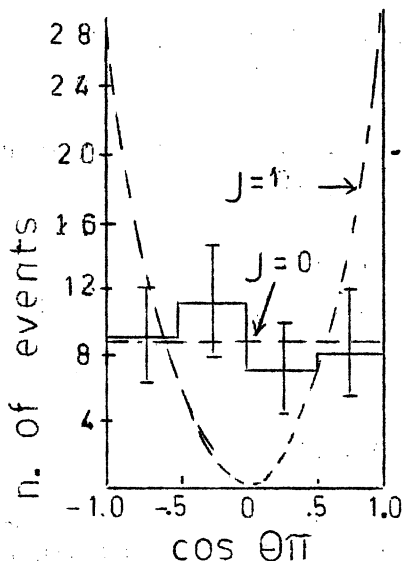


Fig. 17



The spin assignment in question follows:

- the original argument given by Dalitz<sup>7)</sup> and also Dalitz and Liu<sup>8)</sup> which relates the branching ratio  $R_4 = \frac{\pi^- + \text{He}^4}{\text{all modes}}$  to the spin  $J$  and to the p/s ratio in  $\Lambda$  decay;
- an exp. determination of  $R_4$  in nuclear emulsion<sup>9)</sup>;
- the accurate determination of the p/s ratio in  $\Lambda$  decay by Beall et al.<sup>10)</sup> and by Cronin et al.<sup>11)</sup>.

The argument in its essence is the following: the decay  $\Lambda \rightarrow \pi^- + p$  violates parity conservation and can proceed through both

s- and p-wave pion emission (see Dalitz, following lecture). Since the decay  $\Lambda H^4 \rightarrow \pi^- + He^4$  involves spinless particles in the final state, the spin  $J$  of  $\Lambda H^4$  equals the orbital angular momentum  $L$  in the final state.

See fig. 18

Thus, if  $J(\Lambda H^4) = 0$ , the  $\pi$ -r decay will be favoured if s-wave pion emission predominates in  $\Lambda$  decay, being forbidden for zero s-wave amplitude. Conversely,  $J(\Lambda H^4) = 1$ , the  $\pi$ -r decay is forbidden for zero p-wave amplitude and enhanced otherwise.

The experimental value of  $R_4$  found in emulsion is  $0.67 \pm 0.06$ . This combined with the value  $\frac{p^2}{(s)^2 + (p)^2} = 0.11 \pm 0.03$ , and on the basis of the curves calculated by Dalitz and Liu, clearly determines  $J(\Lambda H^4) = 0$ . A more recent determination of  $R_4$  has recently been reported by the He bubble chamber group. Their value,  $0.68 \pm 0.04$ , is in substantial agreement with that mentioned above.

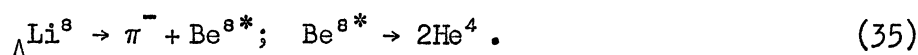
By an entirely similar reasoning  $J = \frac{1}{2}$  has been assigned to  $\Lambda H^3$  (12).

Both angular correlation among the decay products and branching ratios among different final states have enabled a determination of the spin of  $\Lambda Li^8$ . This is the first hypernucleus of the nuclear p-shell for

which such information is available. The ground state of  $\text{Li}^7$  has  $J = 3/2$  while the first excited state of 0.475 MeV has  $J = 1/2$ . The  $\Lambda$  can couple to form  $\Lambda\text{Li}^8$  to either of these states so that a priori the spin of  $\Lambda\text{Li}^8$  could be  $0^-$ ,  $1^-$  or  $2^-$ . The solution of the problem hinges on evidence that the dominant decay



indeed proceeds through intermediate  $\text{Be}^{8*}$  states



The information on the spin is derived from:

- i) the existence of transitions to discrete  $\text{Be}^{8*}$  states and a comparison of the observed with the predicted partial rates for particular final states<sup>13)</sup>;
- ii) the study of the angular correlation between the  $\pi^-$  direction and the  $2\text{He}^4$  direction in their centre of mass.

Values of  $E_{\text{rel}}$  and  $\cos \Theta$  have been calculated for about 43 events<sup>14)</sup>. A plot of  $E_{\text{rel}}$  shows a remarkable grouping of events for  $E_{\text{rel}}$  values of  $\sim 0.1$  MeV,  $\sim 3$  MeV and  $\sim 17$  MeV corresponding to all known levels of  $\text{Be}^{8*}$ .

See fig. 19



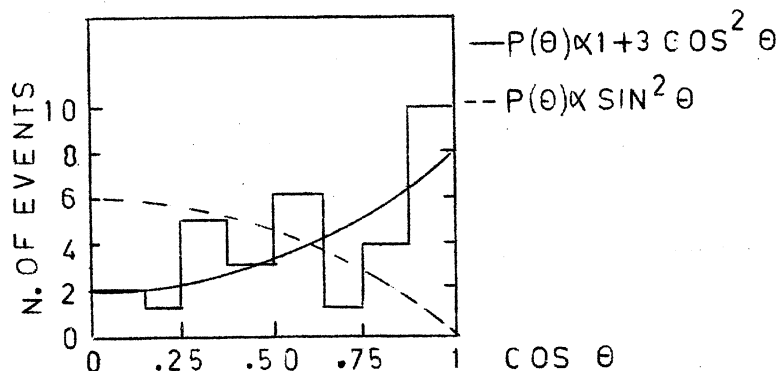
A very small continuum background seems to contribute. The theoretical predictions by Dalitz are based on the following assumptions (simplified here).

- a) The  $\Lambda$ -decay interaction is dominantly s interaction and therefore has odd parity. Thus, any transition via  $\pi^-$  emission to a final state of even parity [like the  $0^+$ ,  $2^+$  ( $T = 0$ ),  $2^+$  ( $T = 1$ ) levels detected here] requires  $l_\pi = \text{odd}$ . Very likely only  $l_\pi = 1$  contributes significantly.
- b) The continuum in the  $E_{\text{rel}}$  distributions is neglected.
- c) The calculations are based on appropriate intermediate-complying nuclear wave functions.

The predictions and the expt. results can be summarized as follows.

	Theory	Expt.
If $J = 2^-$	i) Very small transition rate to $\text{Be}^{8*}$ ( $2^+$ , 3.0 MeV) or $P(\theta) \approx \sin^2 \theta$ for ( $2^+$ ) events	Very large
	ii) Ratio $\frac{2^+, (T=1) \text{ at } 17 \text{ MeV}}{2^+, (T=0) \text{ } 3 \text{ MeV}} \sim 4.5$	4/32
If $J = 1^-$	i) $\frac{2^+(T=0) \text{ } 3.0 \text{ MeV}}{0^+(T=0) \text{ } 0.09 \text{ MeV}} \rightarrow 2.7 - 6.4$	32/5
	ii) $\frac{2^+(T=1) \text{ } 17 \text{ MeV}}{2^+(T=0) \text{ } 3 \text{ MeV}} \sim 0$	4/32
	iii) $P(\theta) \approx 1 + 3 \cos^2 \theta$ for ( $2^+$ ) events	Consistent

Fig. 20



	Theory	Expt.
If $J = 0^-$	Transitions to $0^+$ , $2^+$ states forbidden by angular momentum conservation	Both observed

In conclusion the over-all evidence favours  $J = 1$  for  ${}_{\Lambda}\text{Li}^8$ . This shows that even in the p-shell hypernuclei, as well as in the s-shell ones like  ${}_{\Lambda}\text{H}^3$ ,  ${}_{\Lambda}\text{H}^4$ ,

$$J(\text{HF}) = |(J_1 - 1/2)|$$

where  $J_1$  = spin of the core in its ground state. Purely as an exercise, a calculation of the angular correlation in  ${}_{\Lambda}\text{Li}^8$  decay, assuming  $l_{\pi} = 1$  is appended. This is valid for transitions to the  $2^+$ , 3.0 MeV state of  $\text{Be}^{8*}$ .

As mentioned previously, the study of hypernuclear lifetimes provides us with another check on the spin assignments. Lifetime estimates of some significance are available for  ${}_{\Lambda}\text{H}^3$  and  ${}_{\Lambda}\text{H}^4$ . For  ${}_{\Lambda}\text{He}$  hypernuclei some data have been collected; for heavier hypernuclei no information is available at all. Dalitz and Rajasekharan<sup>15)</sup> have shown that if  ${}_{\Lambda}\text{H}^3$  has spin  $J = 1/2$ , the total decay rate is enhanced considerably. A similar situation occurs if  $J({}_{\Lambda}\text{H}^4) = 0$ . This can be understood qualitatively as due to the fact that if  $J({}_{\Lambda}\text{H}^3) = 1/2$  and  $J({}_{\Lambda}\text{H}^4) = 0$ , the s-channel decay is enhanced by both the Pauli principle, since it leads predominantly to allowed spin configurations, and by the energetic  $(\pi^- + \text{He}^3)$  and  $(\pi^- + \text{He}^4)$  final states respectively. A good estimate of the  ${}_{\Lambda}\text{H}^3$  lifetime is available from the He bubble chamber group experiment<sup>16)</sup>. An estimate of the lifetime of  ${}_{\Lambda}\text{H}^4$  has been reported by Crayton et al.<sup>17)</sup> from an emulsion experiment.

A comparison of the theoretical expectation with the experimental data is given in the following table.

$\tau(\Lambda H^3)$	$J = \frac{1}{2}$	$J = \frac{3}{2}$
Theory	$(1.79 \pm 0.10) \times 10^{-10} \text{ sec}$	$(2.40 \pm 0.03) \times 10^{-10} \text{ sec}$
	$(\tau_\Lambda = 2.35 \times 10^{-10} \text{ sec})$	
Exp.	$(1.05^{+0.20}_{-0.18}) \times 10^{-10} \text{ sec}$	(36 events of which 29 in flight)

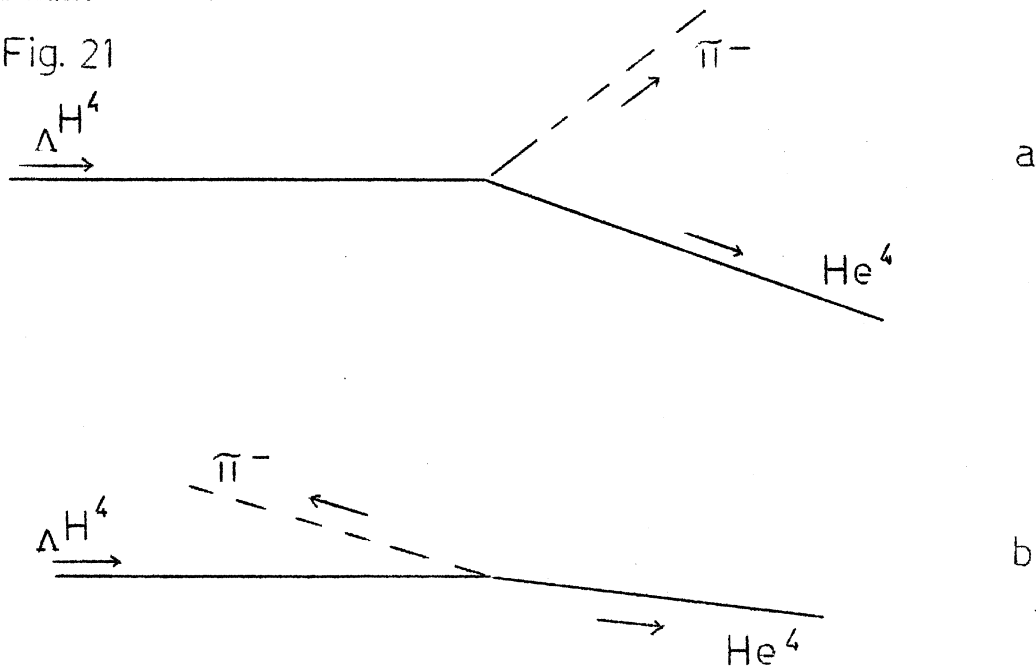
  

$\tau(\Lambda H^4)$	$J = 0$	$J = 1$
Theory	$1.5 \times 10^{-10} \text{ sec}$	$> 2.7 \times 10^{-10} \text{ sec}$
Exp.	$(1.2^{+0.6}_{-0.3}) \times 10^{-10} \text{ sec}$	(52 $\pi$ -r events of which 9 in flight)

The predicted enhancement of the total decay rate for the  $\Lambda$ -n anti-parallel spin orientation has been observed. As a matter of fact the enhancements seem to be even greater than expected at least for  $\Lambda H^3$ , and this may have to be explained.

Examples of  $\Lambda H^4$  decays in emulsion by the  $\pi$ -r mode are shown:

Fig. 21



In a recent study by Ammar et al.<sup>18)</sup> out of 99  $\pi^-$  mesic decay of  $\Lambda^4,^5$  five were found to occur in flight. This yields  $\tau(\Lambda^4,^5) = (1.2_{-0.4}^{+1.0}) \times 10^{-10}$  sec. A result in substantial agreement<sup>19)</sup> based on 51  $\Lambda$ He events of which only four in flight, is again  $\tau(\Lambda^4,^5) = (1.4_{-0.5}^{+1.8}) \times 10^{-10}$  sec.

\* \* \*

#### REFERENCES

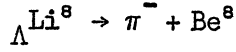
1. R.H. Dalitz and B.W. Downs, Phys.Rev. 111, 967 (1958).
2. R.H. Dalitz, The nuclear interaction of the hyperons, Bangalore Lectures, EFINS 62-9.
3. M. Danyasz and J. Pniewski, Phys.Letters 1, 142 (1962).
4. D.H. Davis, R. Levi-Setti, M. Raymund, O. Skjeggstad, G. Tomasini, J. Lemonne, P. Renard and J. Sacton, Phys.Rev.Letters 2, 464 (1962).
5. T.B. Day and G.A. Snow, Phys.Rev.Letters 2, 59 (1959).
6. M.M. Block, L. Lendinara and L. Monari, Int.Conf.on High-Energy Phys., CERN 1962. p. 371.
7. R.H. Dalitz, Phys.Rev. 112, 605 (1958).
8. R.H. Dalitz and L. Liu, Phys.Rev. 116, 1312 (1959).
9. R.G. Ammar, R. Levi-Setti, W.E. Slater, S. Limentani, P.E. Schlein and P.M. Steinberg, Nuovo Cimento 19, 20 (1961).
10. E.F. Beall, B. Cork, D. Keefe, P.G. Murphy and W.A. Wenzel, Phys.Rev. Letters 8, 75 (1962).
11. J.W. Cronin, Bull.Am.Phys.Soc. 7, 68 (1962).
12. M.M. Block, C. Meltzer, S. Ratti, L. Grimellini, T. Kikuchi, L. Lendinara and L. Monari, Int.Conf.on High-Energy Phys., CERN 1962, p. 458; R.G. Ammar et al. NUPHYS 62104 - in press.

13. R.H. Dalitz, Nucl.Phys. 41, 78 (1963).
14. D.H. Davis, R. Levi-Setti and M. Raymund, Nucl.Phys. - in press, EFINS 62-48.
15. R.H. Dalitz and G. Rajasekharan, Phys.Letters 1, 58 (1962).
16. M.M. Block, C. Meltzer, S. Ratti, L. Grimellini, T. Kikuchi, L. Lendinara and L. Monari, Int.Conf.on High-Energy Phys., CERN 1962, p. 458 and Hyperfragment Conference 1963.
17. N. Crayton, D.H. Davis, R. Levi-Setti, M. Raymund, O. Skjeggestad, G. Tomasini, R.G. Ammar, L. Choy, W. Dunn, M. Holland, J.H. Roberts and E.N. Shipley, Int.Conf.on High-Energy Phys., CERN 1962, p. 460.
18. R.G. Ammar et al., Phys.Letters - in press - NUPHYS 62105.
19. Y.W. Kang, N. Kwak, J. Schneps and P.A. Smith, Hyperfragment Conference 1963.

\* \* \*

APPENDIX

Angular correlation in the decay  $\Lambda \text{Li}^{\ominus} \rightarrow \pi^{-} + \text{Be}^{\ominus}$



$$J \rightarrow 1 \quad 0 \quad 2$$

Fig. 22

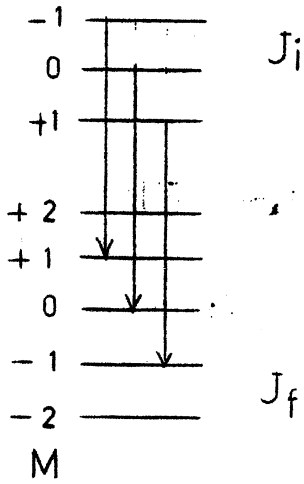
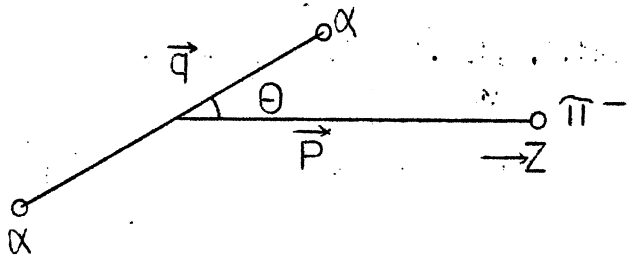


Fig. 23



Take  $l_{\pi} = 1$

$$\omega(\Theta) = \sum_{l_p, l_q} |C(l_p, m_p, l_q, m_q | J, m) Y_{l_p}^m(\hat{p}) Y_{l_q}^m(\hat{q})|^2$$

$$\cos \Theta_p = 1 \quad \cos \Theta_q = \cos \Theta$$

$$Y_{l_p}^m(1) = 0 \quad Y_{l_p}^0(1) = 1$$

$$\omega(\Theta) \sim \sum_{l_p, l_q} |C(l_p, 0, l_q, m_q | j, m) Y_{l_q}^m(\cos \Theta)|^2$$

$$l_p = 1, \quad l_q = 2, \quad j = 1, \quad \Delta m_j = 0$$

$$\omega(\Theta) \sim \sum | \langle 1, 0, 2, M | 1, M \rangle Y_2^M(\cos \Theta) |^2$$

$$M = m = m_q$$

$$M = m_p + m_q$$

$$\omega(\Theta) \sim | \langle 1, 0, 2, 1 | 1, 1 \rangle Y_2^1 |^2 + | \langle 1, 0, 2, 0 | 1, 0 \rangle Y_2^0 |^2 + | \langle 1, 0, 2, -1 | 1, -1 \rangle Y_2^{-1} |^2$$

$$\langle 1, 0, 2, 1 | 1, 1 \rangle = \left[ \frac{(j+M)(j+M+1)}{(2j+1)(2j+2)} \right]^{1/2} = \sqrt{\frac{1}{2}} \quad J = j+1$$

$$\langle 1, 0, 2, 0 | 1, 0 \rangle = \left[ \frac{(j-M+1)(j+M+1)}{(2j+1)(2j+2)} \right]^{1/2} = \sqrt{\frac{2}{3}}$$

$$\langle 1, 0, 2, -1 | 1, -1 \rangle = \left[ \frac{(j-M)(j-M+1)}{(2j+1)(2j+2)} \right]^{1/2} = \sqrt{\frac{1}{2}}$$

$$Y_2^0 = \sqrt{\frac{5}{16\pi}} (3 \cos^2 \Theta - 1)$$

$$Y_2^{\pm 1} = \mp \sqrt{\frac{15}{8\pi}} \sin \Theta \cos \Theta e^{\pm i\varphi}$$

$$Y_2^{\pm 2} = \sqrt{\frac{15}{32\pi}} \sin^2 \Theta e^{\pm 2i\varphi}$$

$$\omega(\Theta) = 2 \frac{1}{2} \frac{15}{8} \sin^2 \Theta \cos^2 \Theta + \frac{2}{3} \frac{5}{16} (9 \cos^4 \Theta - 6 \cos^2 \Theta + 1) =$$

$$\frac{15}{8} \sin^2 \Theta \cos^2 \Theta + \frac{15}{8} \cos^4 \Theta - \frac{30}{24} \cos^2 \Theta + \frac{5}{24} = \frac{5}{24} (1 + 3 \cos^2 \Theta) .$$

Case 2 → 2

$$\omega(\Theta) = 2 |\langle 1, 0, 2, 2 | 2, 2 \rangle Y_2^2|^2 + 2 |\langle 1, 0, 2, 1 | 2, 1 \rangle Y_2^1|^2$$

$$+ |\langle 1, 0, 2, 0 | 2, 0 \rangle Y_2^0|^2 \rightarrow \sim \sin^2 \Theta .$$

\* \* \*



Table 1  
Binding energies from uniquely identified mesonic decays †)  
March, 1963

Identity	Decay mode	$\bar{B}_\Lambda$ (MeV)	$\sigma_{av}^{*})$ (MeV)	$\sigma$ (MeV)	No. of events
$\Lambda^H^3$	$\pi - r$	0.38	0.24	$1.05 \pm 0.16$	20
	all other	0.27	0.19	$0.80 \pm 0.15$	18
	total	0.31	0.15	-	38
$\Lambda^H^4$	$\pi - r$	2.40	0.12	$0.99 \pm 0.10$	62
	n	1.75	0.18	$0.82 \pm 0.13$	20
	all other	2.00	0.14	$0.71 \pm 0.10$	27
	total	2.14	0.08	-	109
$\Lambda^He^4$	all	2.47	0.09	$0.61 \pm 0.008$	48
$\Lambda^He^5$	all	3.10	0.05	$0.57 \pm 0.04$	147
$\Lambda^He^7$	all	3.96	-	$0.9 \pm 0.2$	14
$\Lambda^Li^9$	$\pi - r$	5.51	-	$1.0 \pm 0.3$	9
	all other	5.52	0.12	$0.45 \pm 0.08$	16
$\Lambda^Li^8$	all	6.65	0.15	$1.06 \pm 0.12$	44
$\Lambda^Li^9$	$\pi - r$	6.9	0.8	inferred	1
	all other	8.01	0.29	-	9
$\Lambda^Be^7$	all	4.9	0.5	inferred	2
$\Lambda^Be^8$	all	6.35	0.30	inferred	4
$\Lambda^Be^9$	all	6.50	0.16	$0.30 \pm 0.06$	10
$\Lambda^Be^{10}$	$\pi - r$	9.48	-	$1.0 \pm 0.4$	4
	all other	8.36	0.6	inferred	1
$\Lambda^B^{10}$	$\pi - r$	10.0	-	$1.0 \pm 0.3$	6
$\Lambda^B^{11}$	$\pi - r$	10.0	-	$0.6 \pm 0.2$	4
	all other	9.9	0.6	inferred	1
$\Lambda^B^{12}$	all	10.50	0.18	$0.6 \pm 0.15$	8
$\Lambda^C^{13}$	$\pi - r$	10.6	0.4	inferred	2
$\Lambda^C^{14}$	$\pi - r$	13.2	0.7	inferred	1
$\Lambda^N^{14}$	$\pi - r$	11.7	0.5	inferred	1

\*) Possible systematic errors ( $\pm 0.2$  MeV) have not been included.

†) Computed from the data contained in the enclosed references.

REFERENCES to Table 1

- R.G. Ammar, R. Levi-Setti, W.E. Slater, S. Limentani, P.E. Schlein and P.H. Steinberg, *Nuovo Cimento* 15, 181 (1960).
- R.G. Ammar, R. Levi-Setti, W.E. Slater, S. Limentani, P.E. Schlein and P.H. Steinberg, *Nuovo Cimento* 19, 20 (1961).
- P.E. Schlein and W.E. Slater, *Nuovo Cimento* 21, 213 (1961).
- R. Levi-Setti, W.E. Slater and V.L. Telegdi, *Nuovo Cimento* 10, 68 (1958); contains previous literature.
- S. Mora and I. Ortalli, *Nuovo Cimento* 12, 635 (1959).
- G.C. Deka, *Nuovo Cimento* 14, 1217 (1959).
- S. Lokanathan, D.K. Robinson and S.J. St. Lorant, *Proc. Roy. Soc. (London)* A254, 470 (1960).
- J. Sacton, *Nuovo Cimento* 15, 110 (1960).
- J. Tietge, *Nucl. Phys.* 20, 227 (1960).
- M. Taher-Zadeh, *Nuovo Cimento* 17, 980 (1960).
- M.M. Nikolić, *Nucl. Phys.* 21, 595 (1961).
- Y. Prakash, P.H. Steinberg, D.A. Chandler and R.J. Prem, *Nuovo Cimento* 21, 235 (1961).
- M.J. Beniston and D.H. Davis, *Phil. Mag.* 7, 2119 (1962) and private communication.
- N. Crayton, R. Levi-Setti, M. Raymund, O. Skjeggstad, D. Abeledo, R.G. Ammar, J.H. Roberts and E.N. Shipley, *Rev. Mod. Phys.* 34, 186 (1962).
- W. Gajewski, J. Pniewski, T. Pniewski and S. Popov (to be published), quoted in J. Pniewski and M. Danysz, *Phys. Letters* 1, 142 (1962);  $1 \Lambda \text{He}^7$  event.
- A.A. Varfolomev, R.I. Gerasimova and L.A. Karpova, *Soviet Phys. Doklady* 1, 579 (1956), *DAN* 110, 758 (1956);  $1 \Lambda \text{He}^7$  event.
- S.J. St. Lorant, private communication,  $1 \Lambda \text{Be}^7$  event.
- R.G. Ammar, M. Holland, J.H. Roberts and E.N. Shipley, *Nuovo Cimento* 27, 769 (1963);  $1 \Lambda \text{Be}^7$  event.

D.J. Prowse, Bull. Am. Phys. Soc. II, 7, 297 (1962), and private communication June 1962; 1  $\Lambda N^{14}$  event.

A.Z. Ismail, I. Kenyon, A. Key, S. Lokanathan and Y. Prakash, Nuovo Cimento 27, 1228 (1963); 3  $\Lambda He^7$ , 1  $\Lambda Li^7$ , 1  $\Lambda Li^8$  and 2  $\Lambda B^{12}$  events.

R.G. Ammar, L. Choy, W. Dunn, M. Holland, J.H. Roberts, E.N. Shipley, N. Crayton, D.H. Davis, R. Levi-Setti, M. Raymund, O. Skjeggestad and G. Tomasini, Nuovo Cimento 27, 1078 (1963).

D.H. Davis, R. Levi-Setti and M. Raymund, Nucl. Phys. 41, 73 (1963).

\* \* \*

## DISCUSSION

- Rao : I would like to know why the lighter of the decay products of the hyperfragments is generally taken as a  $\pi^-$  meson.
- Levi-Setti : We can say that the so-called  $\pi$  meson is indeed a  $\pi^-$  meson in perhaps 60% of the cases because we do observe a  $\sigma$  star, a capture star which can only be characteristic of  $\pi^-$  mesons and not of captured  $\mu^-$  mesons, for instance. Of course, there are a large number of cases in which the  $\pi^-$  stops without producing any visible star and then the question is open if that particle is indeed a pion or not. In general in the large majority of cases one has obtained a satisfactory momentum balance for such identification and with this evidence one is satisfied with the interpretation of it being a pion. One would expect that if the particle was indeed, for instance, a  $\mu$  meson, this would lead to noticeable anomalies in the decay. This, of course, suggests that it may be worth while to actually measure the mass of the particle which is emitted when this leads to a so-called  $\rho$  ending. A further consideration is that, as we know,  $\mu^-$  at rest in emulsion  $\beta$  decay in a sizeable fraction of the cases so that if indeed a  $\mu^-$  is emitted one would very much like to see the decay electron to support this conclusion.
- Spitzer : Is there any success in the search for  $\pi^0$  mesic decays, and why, if you count these decays among the mesic decays, is there no correction in the production rate of the mesic hyperfragments for the unseen  $\pi^0$  mesic decays?
- Levi-Setti :  $\pi^0$  mesic decays have been occasionally observed in emulsion. In two or three examples Dalitz pairs have been observed. There has been a systematic analysis made in Chicago of  $\pi^0$

- Levi-Setti : decays by measuring those events in which only a recoil  
(cont.) was visible. This turned out in the identification of a number of two-body decays of  $\Lambda \text{He}^4$  by the  $\pi^0$  mode. I would like, however, to say that it is a lost cause to try to do any work on  $\pi^0$  decays in emulsion. I think that the He bubble chamber has given exceedingly good results on  $\pi^0$  modes for  $\Lambda \text{H}$  and  $\Lambda \text{He}$ , certainly more reliably than could ever be achieved in emulsion. For  $\pi^0$  decays of heavier species, of course, the emulsion would be the only way, but in view of the difficulties encountered even in the  $\pi^-$ -mesic decays (if you take away the pion, you observe only a blob), I would say that in general, they would be undetected.
- Hoogland : There exists some different range momentum curves and you showed the Wilkins' normalized curves. I know that different groups are using them and I think that for a rather heavy fragment this can give rise to some differences in interpretation of the hyperfragments. Does there exist some normalization in the use of these curves?
- Levi-Setti : The slide I have shown is an old slide of several years ago. Now we use the Barkas heavy ion range-energy curves. To some extent if you have a large body of events, this becomes somewhat irrelevant because you can actually obtain a best fit to an empirical range-energy curve for  $\text{He}^4$  and from that derive the curve for the other isotopes. In all cases there is a good normalization point which one can obtain from the  $\pi$ -r decays of  $\Lambda \text{H}^4$ . Any experimental curve for  $\text{He}^4$  will have to intercept this calibration point.
- Renard : What is the situation about the experimental difference in binding energy of  $\Lambda \text{H}^4$  and  $\Lambda \text{He}^4$ ?
- Levi-Setti : Taking the  $\Lambda \text{H}^4$   $\pi$ -r modes the binding energy is 2.40, to be compared with  $\Lambda \text{He}^4$  for which the average binding is 2.47 MeV. (See Table 1.)

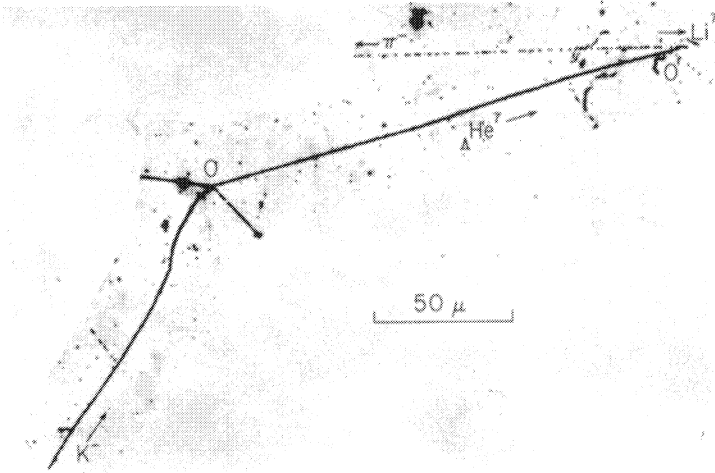


Fig. 2. Example of  ${}^7_2\text{He} \rightarrow {}^7_3\text{Li} + \pi^-$

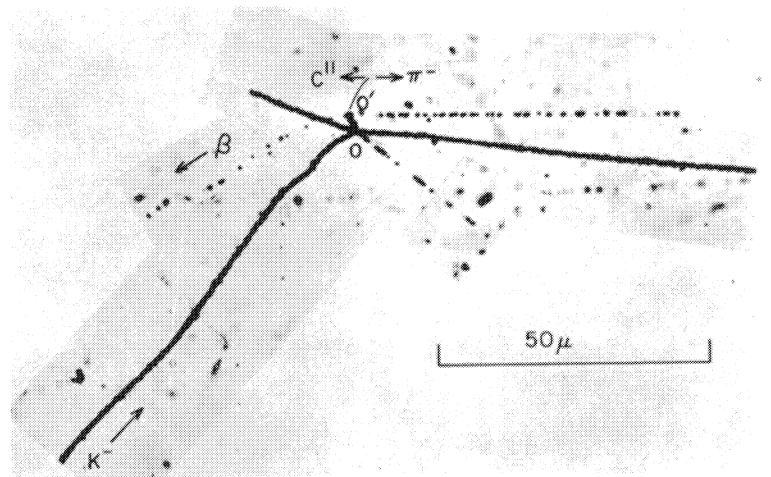


Fig. 3. Example of  ${}^{11}_5\text{B} \rightarrow \pi^- + {}^{11}_6\text{C} + \beta^+$

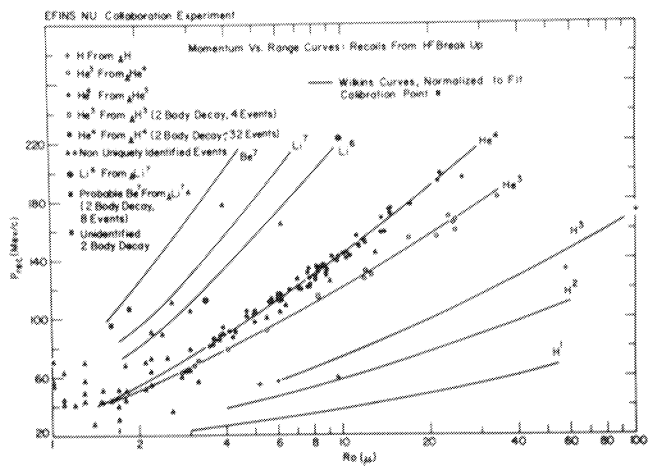


Fig. 4. Plot of recoil momentum against range.

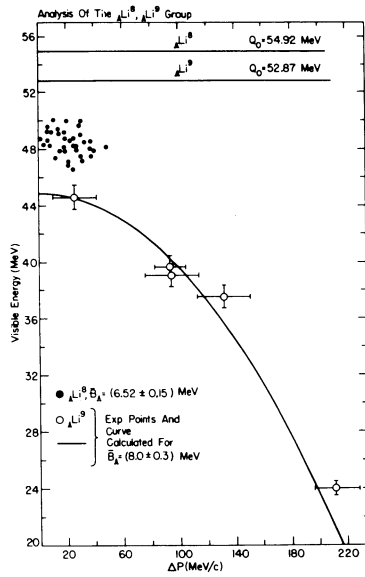


Fig. 6. Energy release  $Q$  versus missing momentum ( $\Delta P$ ) for  $\text{Li}^8$  and  $\text{Li}^9$  events.

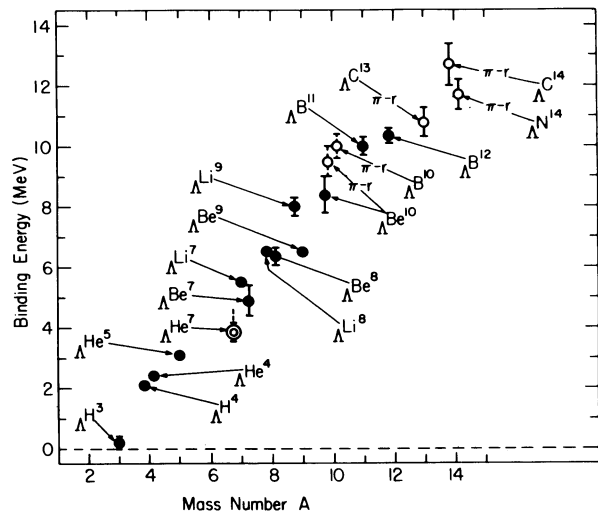


Fig. 8. Binding energy versus Mass Number.

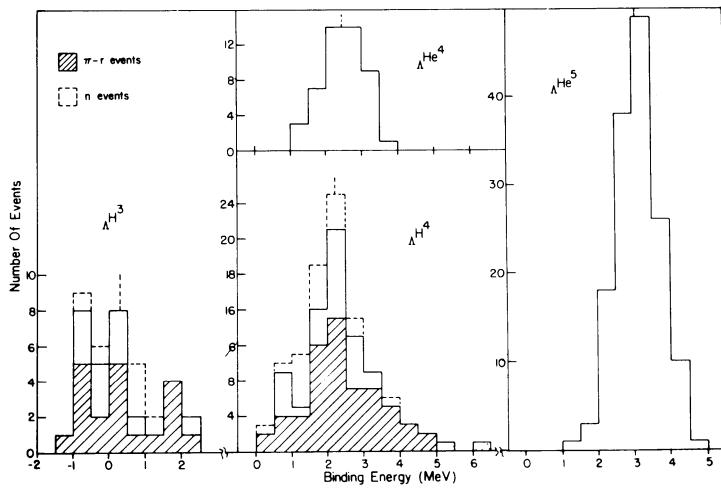


Fig. 9. Binding energies of  $\Lambda \text{H}^3$ ,  $\Lambda \text{He}^4$ ,  $\Lambda \text{H}^4$  and  $\Lambda \text{He}^5$ .

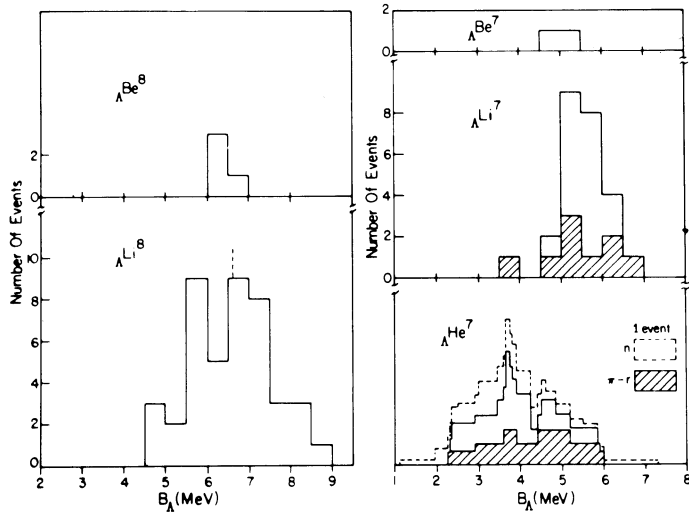


Fig. 10. Binding energies of  ${}^{\Lambda}\text{Be}^7$ ,  ${}^{\Lambda}\text{Li}^7$ ,  ${}^{\Lambda}\text{He}^7$ ,  ${}^{\Lambda}\text{Be}^8$  and  ${}^{\Lambda}\text{Li}^8$ .

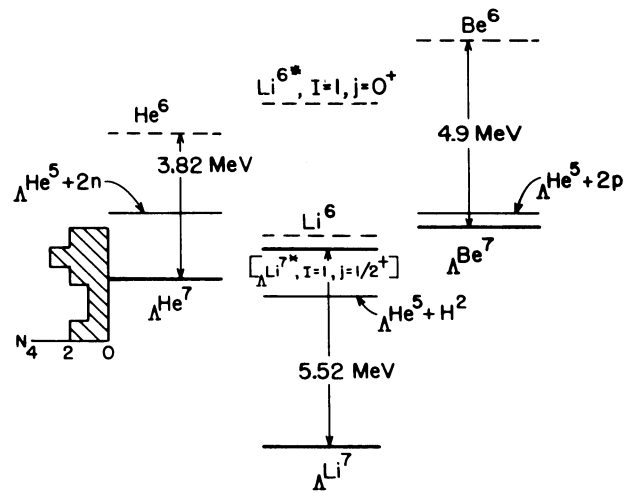


Fig. 11. Energy level diagram.

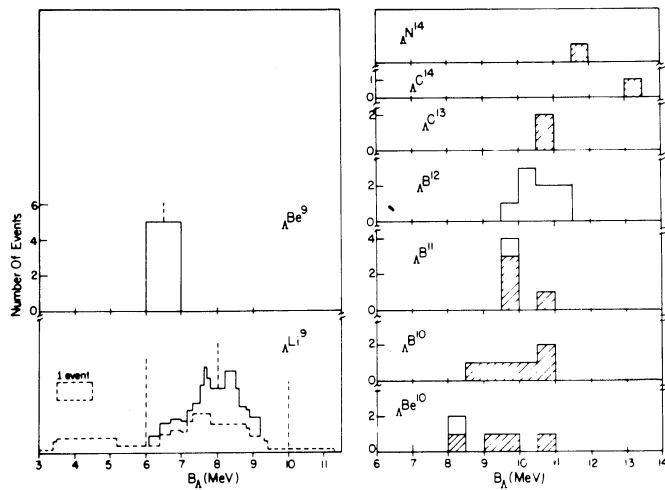


Fig. 12. Binding energies of Li, Be, B, C, and H hypernuclei.



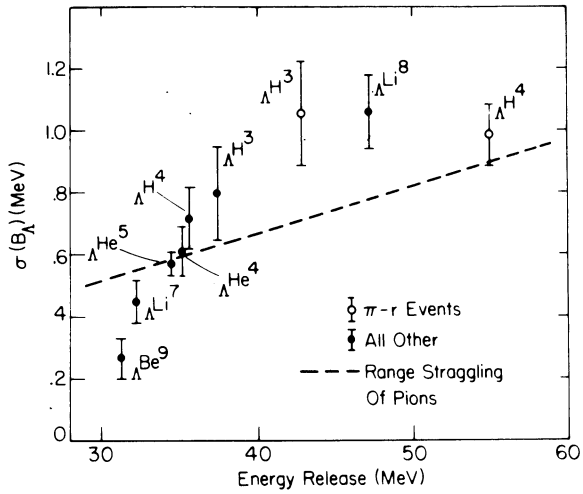


Fig. 13. Spread  $\sigma$  of  $B_\Lambda$  distributions as a function of the energy release  $Q$ .

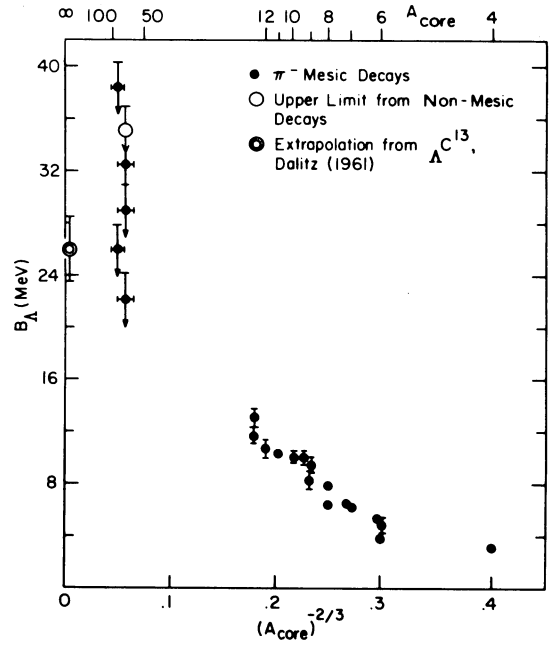


Fig. 15.  $B_\Lambda$  versus  $A^{-2/3}$ .

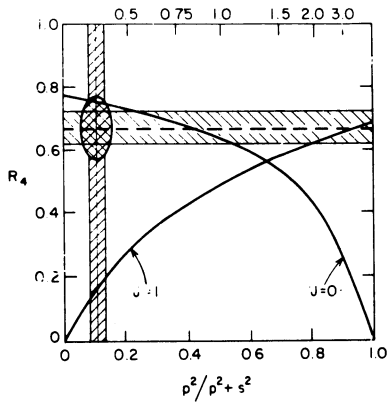


Fig. 18. The branching ratio  $R = (\text{He}^4 + \pi^-)/(\text{all } \pi^- \text{ modes})$  for  $\Lambda \text{H}^4$  decay is compared with the calculated ratios for  $\Lambda \text{H}^4$  spin  $J = 0$  and  $J = 1$ , and with the measured value  $p^2/(p^2 + s^2) = 0.11 \pm 0.03$ .

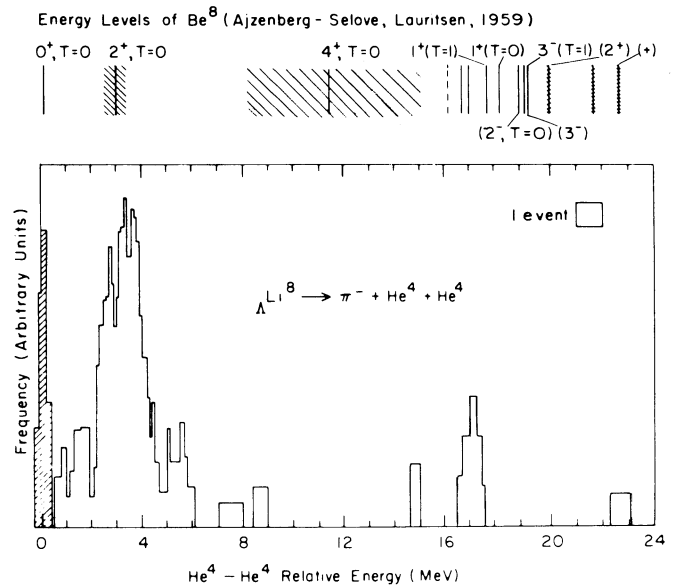


Fig. 19. Plot of  $\text{He}^4 - \text{He}^4$  relative energy for  $\text{Li}^8 \rightarrow \pi^- + \text{He}^4 + \text{He}^4$ .